The Activation of Natural Killer T Cells Ameliorates Post-Infarct Cardiac Remodeling and Failure in Mice

Mochamad Ali Sobirin, MD, PhD; Shintaro Kinugawa, MD, PhD; Masashige Takahashi, MD; Arata Fukushima, MD; Tsuneaki Homma, MD; Taisuke Ono, MD; Kagami Hirabayashi, MD, PhD; Tadashi Suga, BS; Putri Azalia, MD; Shingo Takada, BS; Masaru Taniguchi, MD, PhD; Toshinori Nakayama, MD, PhD; Naoki Ishimori, MD, PhD; Kazuya Iwabuchi, MD, PhD; and Hiroyuki Tsutsui, MD, PhD

Department of Cardiovascular Medicine, Hokkaido University Graduate School of Medicine, Sapporo (M.A.S, S.K., M.T., A.F., T.H., T.O., K.H., T.S., P.A., S.T., N.I., H.T.); Faculty of Medicine, Diponegoro University, Semarang, Indonesia (M.A.S); RIKEN Research Center for Allergy and Immunology, Kanagawa, Japan (M.T.); Department of Immunology, Graduate School of Medicine, Chiba University, Chiba, Japan (T.N.); Division of Immunobiology, Kitasato University School of Medicine, Kanagawa, Japan (K.I.).

Short title: Natural killer T cells in heart failure

Address correspondence: Shintaro Kinugawa, MD, PhD
Department of Cardiovascular Medicine, Hokkaido University Graduate School of Medicine, Kita-15, Nishi-7, Kita-ku, Sapporo 060-8638, Japan
Fax number: +81-11-706-7874,
Tel number: +81-11-706-6973
E-mail address: tuckahoe@med.hokudai.ac.jp

Word length: 6813 words, **Number of references**: 42, **Number of figures**: 8
Journal subject codes: [110][115][147][148]

Abstract

Rationale: Chronic inflammation in the myocardium is involved in the development of left ventricular (LV) remodeling and failure after myocardial infarction (MI). Invariant natural killer T (iNKT) cells have been shown to produce inflammatory cytokines and orchestrate tissue inflammation. However, no previous studies have determined the pathophysiological role of iNKT cells in post-MI LV remodeling.

Objective: The purpose of this study was to examine whether the activation of iNKT cells might affect the development of LV remodeling and failure.

Methods and Results: After creation of MI, mice received the injection of either α-galactosylceramide (αGC; n=27), the activator of iNKT cells, or phosphate-buffered saline (PBS; n=31) 1 and 4 days after surgery, and were followed during 28 days. Survival rate was significantly higher in MI+αGC than MI+PBS (59% vs 32%, $P<0.05$). LV cavity dilatation and dysfunction were significantly attenuated in MI+αGC, despite comparable infarct size, accompanied by a decrease in myocyte hypertrophy, interstitial fibrosis, and apoptosis. The infiltration of iNKT cells were increased during early phase in non-infarcted LV from MI and αGC further enhanced them. It also enhanced LV interleukin (IL)-10 gene expression at 7 days, which persisted until 28 days. Anti IL-10 receptor antibody abrogated these protective effects of αGC on MI remodeling. The administration of αGC into iNKT cell-deficient $J\alpha18^{-/-}$ mice had no such effects, suggesting that αGC was a specific activator of iNKT cells.

Conclusions: iNKT cells play a protective role against post-MI LV remodeling and failure through the enhanced expression of cardioprotective cytokines such as IL-10.

Key words: invariant natural killer T cells, myocardial infarction, inflammation, heart failure, cytokines.

Non-standard Abbreviations and Acronyms	
αGC	α-galactosylceramide
HF	heart failure
IL	Interleukin
IFN-γ	interferon-γ
iNKT	invariant natural killer T
LV	left ventricle
MI	myocardial infarction
MCP-1	monocyte chemoattractant protein-1
MMP	matrix metalloproteinase
NK	natural killer
PBS	phosphate-buffered saline
qRT-PCR	quantitative reverse transcriptase-polymerase chain reaction
RANTES	regulated on activation normally T cell expressed and secreted
T_H1	T-helper type 1
T_H2	T-helper type 2
TNF-α	tumor necrosis factor-α

Introduction

Myocardial infarction (MI) leads to the development of heart failure (HF), which is the major cause of death in post-MI patients. The changes in left ventricular (LV) geometry, such as cavity dilatation associated with myocyte hypertrophy and interstitial fibrosis, referred to as remodeling, contribute to the development of depressed cardiac function in HF after MI.[1] It has been reported that monocytes and lymphocytes are infiltrated in non-infarcted area as well as infarcted area of LV after MI.[2, 3] Chemokines, monocyte chemoattractant protein-1 (MCP-1) and regulated on activation normally T cell expressed and secreted (RANTES), are essential factors in the recruitment and activation of monocyte and lymphocyte. These chemokines are also increased in non-infarcted LV after MI and contribute to local inflammation through the release of inflammatory cytokines including tumor necrosis factor-α (TNF-α).[2, 4] Targeted deletion of CC chemokine receptor 2 or anti-MCP-1 gene therapy has been shown to attenuate LV remodeling after MI.[2, 5] Thus, chronic tissue inflammation plays an important role in LV remodeling process.

Invariant natural killer T (iNKT) cells are innate-like T lymphocyte population co-expressing NK markers and an αβ T cell receptor that recognize glycolipid antigens. They can rapidly and robustly produce a mixture of T-helper type 1 (T_H1) and T_H2 cytokines, such as TNF-α, interferon-γ (IFN-γ), interleukin (IL)-10, and IL-4, and also a vast array of chemokines in shaping subsequent adaptive immune response.[6] Thus, iNKT cells can function as a bridge between the innate and adaptive immune systems, and orchestrate tissue inflammation. Indeed, we have shown that iNKT cells activate vascular wall inflammation in atherogenesis and adipose tissue inflammation in obesity-induced glucose intolerance.[7, 8] On the other hand, iNKT cells play a protective role against autoimmune and inflammatory diseases such as type 1 diabetes,[9, 10] allergic encephalomyelitis,[9, 11] and rheumatoid arthritis.[12] These findings suggest that iNKT cells may have bidirectional effects on tissue inflammation. However, no previous studies have examined the changes of iNKT cells and their pathophysiological role in LV remodeling and failure after MI.

Therefore, the purpose of the present study was to determine whether iNKT cells might affect the development of LV remodeling and failure after MI. We demonstrated that the activation of iNKT cells by α-galactosylceramide (αGC), a specific activator for iNKT cells,[13] attenuated the development of LV remodeling and failure after MI in mice. The enhanced gene expression of IL-10 might be involved in these beneficial effects of iNKT cells on this disease process.

Methods

All procedures and animal care were approved by our institutional animal research committee and conformed to the animal care guideline for the Care and Use of Laboratory Animals in Hokkaido University Graduate School of Medicine.

Experiment 1: Time-dependent Changes of iNKT Cell Receptors in Post-MI Hearts

Animal Models

MI was created in male C57BL/6J mice, 6-8 weeks old and 20 to 25 g body weight, by ligating the left coronary artery as described previously.[14] Sham operation without ligating the coronary artery was also performed as control. MI mice were sacrificed and the hearts were excised at day 3, 7, 14 and 28 for quantitative reverse transcriptase-polymerase chain reaction (qRT-PCR) measurements.

qRT-PCR

Quantitative PCR for Vα14Jα18 (a specific marker of iNKT cells) was performed, as described previously.[8]

Experiment 2: Effects of iNKT Cell Activation on Post-MI Hearts

Animal Models

Sham and MI mice were created in male C57BL/6J as described in Experiment 1. Each group of mice was randomly divided into 2 groups; either αGC (0.1μg/g body weight; Funakoshi Company, Ltd., Tokyo, Japan), the activator of iNKT cells, or phosphate-buffered saline (PBS) was administered via intraperitoneal injection 1 and 4 days after surgery. The concentration of αGC was chosen based on the previous study of its efficacy.[8] Thus, the experiment was performed in the following 4 groups of mice; sham+PBS (n=10), sham+αGC (n=10), MI+PBS (n=31), and MI+αGC (n=27).

Survival

The survival analysis was performed in all 4 groups of mice. During the study period, the cages were inspected daily for deceased animals. All deceased mice were examined for the presence of MI as well as pleural effusion and cardiac rupture.

Echocardiographic and Hemodynamic Measurements

Echocardiographic and hemodynamic measurements were performed under light anesthesia with tribromoethanol/amylene hydrate (avertin; 2.5% wt/vol, 8 μL/g ip), as described previously.[14]

Myocardial Histopathology, Infarct Size, Myocardial Apoptosis, and Matrix Metalloproteinase (MMP) Zymography

Myocyte cross-sectional area, collagen volume fraction, infarct size, myocardial apoptosis, and zymographic MMPs levels were determined as described previously.[14, 15]

Isolation of Cardiac Mononuclear Cell and Flow Cytometry

Cardiac mononuclear cells from 3 mice were isolated, pooled, and subjected to flow cytometric analysis as previously described.[7, 16]

qRT-PCR

Quantitative PCR for Vα14Jα18, CD11c (a marker of M1 macrophages), arginase-1 (a marker of M2 macrophages), MCP-1, RANTES, IFN-γ, IL-4, IL-6, TNF-α, and IL-10 was performed, as described previously.[8]

Immunohistochemistry

LV sections were immunostained with antibody against mouse MAC3 (a macrophage marker), mouse CD3 (a T cell marker), or mouse myeloperoxidase (a leucocyte marker), followed by counter-staining with hematoxylin.

Plasma Cytokines Concentration

Plasma IL-10, TNF-α, IFN-γ, IL-6, and IL-4 levels were measured by commercially available ELISA kit (R&D systems, Inc.) in all groups.

Experiment 3: Effects of IL-10 Neutralization on αGC-Treated Post-MI Hearts

MI mice were divided into the following 3 goups; MI+αGC (n=18), MI+anti-IL-10 receptor antibody (n=12), and MI+αGC+anti-IL-10 receptor antibody (n=19). αGC was administered identically as in Experiment 2. Anti-IL-10 receptor antibody (500μg/mouse, BD Pharmingen, San Diego, CA) was administered via intraperitoneal injection 1, 4, and 14 days after surgery. The concentration of anti-IL-10 receptor antibody was chosen based on the previous study of its efficacy.[12] Four weeks after surgery, echocardiographic and hemodynamics measurement were performed. Separate groups of mice were used in MI+αGC group in Experiment 2.

Experiment 4: Specificity of αGC for NKT Cells

$V\alpha14^{+}$ NKT cell-deficient $J\alpha18^{-/-}$ (Jα18 KO) mice were provided from Dr. M. Taniguchi (RIKEN, Yokohama, Japan) and backcrossed 10 times to C57BL/6J.[17] Sham and MI mice were

created in male Jα18 KO mice as described in Experiment 1. Each group of mice was treated identically to Experiment 2. Thus, the experiment was performed in the following 4 groups; KO+sham+PBS, KO+sham+αGC, KO+MI+PBS, and KO+MI+αGC. One week after surgery, all mice (n=9 for each group) were sacrificed, and used for immunohistochemistry (n=3 for each group), and for qRT-PCR (n=6 for each group). These analyses were performed as described in Experiment 2.

Statistical Analysis

Data were expressed as means ± SE. Survival analysis was performed by the Kaplan-Meier method, and between-group differences in survival were tested by the log-rank test. A between-group comparison of means was performed by 1-way ANOVA, followed by t test. The Bonferroni correction was applied for multiple comparisons of means. $P<0.05$ was considered statistically significant.

The authors had full access to and take full responsibility for the integrity of the data. All authors had read and agreed to the manuscript as written.

Results

Experiment 1: Time-dependent Changes of iNKT Cell Receptors in Post-MI Hearts

The quantification of iNKT cells by Vα14/Jα18 gene expression demonstrated that iNKT cell infiltration into the non-infarcted LV was significantly enhanced at 7 days (1.7±0.2 fold changes from baseline, P<0.05 vs. baseline) after MI and returned to baseline at 14 and 28 days after MI (1.0±0.2 and 1.1±0.1 fold changes from baseline, respectively). In the infarcted LV, its gene expression was significantly elevated 7 days and remained elevated 28 days after MI (data not shown).

Experiment 2: Effects of iNKT Cell Activation on Post-MI Hearts

By using flow cytometric analysis, iNKT cells were detected in LV from all groups of mice (**Figure 1A**). αGC injection increased iNKT cells infiltration into the non-infarcted LV both in sham+αGC and MI+αGC mice after 7 days (**Figure 1A**). Moreover, it remained enhanced at 28 days in MI+αGC (**Figure 1A**).

Quantitative RT-PCR also demonstrated that gene expression of Vα14/Jα18, a marker of iNKT cell infiltration, was significantly elevated in the non-infarcted LV from sham+αGC and MI+αGC mice after 7 days (**Figure 1B**). Interestingly, it remained significantly increased at 28 days only in MI+αGC (**Figure 1B**).

Survival

There were no deaths in sham-operated groups. The survival rate during 28 days was significantly higher in MI+αGC compared with MI+PBS mice (59 % versus 32 %; *P*<0.05; **Figure 2A**). Thirteen MI+PBS (42%) and 8 MI+αGC (30%) mice died of LV rupture (*P*=NS).

Echocardiography and Hemodynamics

The echocardiographic and hemodynamic data from 4 groups of survived mice at 28 days are shown in **Figure 2B** and **Table 1**. There were no significant differences in either echocardiographic or hemodynamic parameters between sham+PBS and sham+αGC mice. LV diameters were significantly greater, and LV fractional shortening was significantly lower in MI mice than sham mice. These changes were ameliorated by the treatment of MI mice with αGC. There were no significant differences in heart rate or aortic blood pressure among groups. LV end-diastolic pressure (LVEDP) was significantly increased, and LV +dP/dt and LV –dP/dt were significantly decreased in MI compared to sham, which was ameliorated by the treatment of MI mice with αGC.

Organ Weights, Infarct Size, and Histology

There were no significant differences in heart weight/body weight and lung weight/body

weight between sham+PBS and sham+αGC mice (**Table 1**). In agreement with LVEDP, heart weight/body weight and lung weight/body weight were increased in MI mice, and these increases were significantly attenuated in MI+αGC (**Table 1**).

Infarct size measured by the morphometric analysis was comparable (56±2% versus 55±1%; *P*=NS) between MI+PBS (n=6) and MI+αGC (n=6) groups (**Table 1**).

Histomorphometric analysis of noninfarcted LV sections showed that myocyte cross-sectional area was increased in MI+PBS compared to sham mice, and was significantly attenuated in MI+αGC (**Figure 3A**). Collagen volume fraction was also increased in MI+PBS compared to sham mice, and was significantly attenuated in MI+αGC (**Figure 3A**).

There were rare TUNEL-positive nuclei in both sham and sham+αGC mice. The number of TUNEL-positive myocytes in the noninfarcted LV was increased in MI+PBS, and was significantly decreased in MI+αGC (**Figure 3B)**.

Myocardial MMP Activity

Representative gelatin zymography of the non-infarcted LV tissue at day 7 from 4 groups of mice was shown in **Figure 4A**. There were no zymographic MMP-2 and 9 levels in the sham+PBS and sham+αGC. Zymographic MMP-2 level was significantly increased in MI+PBS mice compared to sham mice at day 7. αGC injection significantly decreased it after MI (**Figure 4B**). Zymographic MMP-9 level was also increased in MI+PBS mice compared to sham mice at day 7, which, however, was not affected by αGC (**Figure 4C**).

Zymographic MMP-2 level was increased in MI+PBS mice also at day 28, and αGC injection tended to decrease it (3.7±1.1 vs 2.1±0.8 in ratio to sham, P=0.08).

Inflammatory and Cytokine Gene Expression

Immunohistochemical stainings for MAC3 and CD3 were increased in MI+PBS compared to Sham+PBS, and were further increased by αGC at day 7 (**Figure 5**). MPO positive cells were not detected in the LV tissue from either group of mice (data not shown).

CD11c (a marker of M1 macrophage) and arginase 1 (a marker of M2 macrophage) gene expressions were significantly increased in non-infarcted LV from MI+PBS compared to sham+PBS at day 7 (**Figure 6A and B**). αGC significantly increased their expressions in both sham and MI animals at day 7. Arginase 1, but not CD11c, was increased in non-infarcted LV from MI+PBS and MI+αGC at day 28. There was no significant difference in arginase 1 between these 2 groups. MCP-1 and RANTES gene expressions were increased in non-infarcted LV from MI+PBS compared to sham+PBS at day 7 (**Figure 6C and D**). αGC significantly increased their expressions in both sham and MI animals at day 7. In contrast, there was no significant difference in their expressions among all groups at day 28.

IFN-γ, TNF-α, IL-6, and IL-10 gene expression levels were significantly increased in sham and MI mice by αGC at day 7 (**Figure 6E-H**). IL-10 gene expression alone significantly elevated up to 2.6 fold in the non-infarcted LV from MI+αGC mice at day 28 (**Figure 6H**). These time-dependent and αGC-mediated changes in IL-10 gene expression (**Figure 6H**) in the LV were matched with those in NKT cell infiltration (**Figure 1B**). IL-4 was not detected in either group.

Plasma Cytokines Concentration

Plasma IL-10 level was similar among sham+PBS, sham+αGC, and MI+PBS groups (9.0±0.5 vs 9.8±2.3 vs 10.6±2.3 pg/ml). However, in parallel to IL-10 gene expression in the LV, it significantly increased up to 2-fold in MI+αGC (21.1±2.3 pg/ml) compared with sham and MI+PBS mice ($P<0.05$). Plasma IFN-γ level was similar among 4 groups of mice (1.4±0.3 vs 1.7±0.3 vs 0.9±0.2 vs 1.0±0.2 pg/ml, P=NS). Plasma TNF-α, IL-6, and IL-4 levels were not detected in either group.

Experiment 3: Effects of IL-10 Neutralization on αGC-Treated Post-MI Hearts

Survival

The survival rate during 28 days tended to be higher in MI+αGC than MI+anti-IL-10 receptor antibody and MI+αGC+anti-IL-10 receptor antibody (66.7 % versus 44.4 % and 42.1%, P=0.4).

Echocardiography and Hemodynamics

The echocardiographic and hemodynamic data from 3 groups of surviving mice are shown in **Table 2**. IL-10 receptor antibody injection significantly increased LV diameters, LVEDP, and decreased LV fractional shortening in αGC-treated MI mice. In contrast, there were no differences in these parameters between MI+anti-IL-10 receptor antibody and MI+αGC+anti-IL-10 receptor antibody. There was no significant difference in heart rate and aortic blood pressure among 3 groups.

Organ Weights and Infarct Size

In agreement with LVEDP, lung weight/body weight ratio was significantly increased in MI+αGC +anti-IL-10 receptor antibody compared to MI+αGC (**Table 2**). There were also no differences in these parameters between MI+anti-IL-10 receptor antibody and MI+αGC+anti-IL-10 receptor antibody.

Infarct size was comparable (56±2%, 54±2%, and 56±4%; *P*=NS) among MI+αGC (n=8), MI+anti-IL-10 antibody (n=8), and MI+αGC+anti-IL-10 receptor antibody (n=8) groups.

Experiment 4: Specificity of αGC for iNKT cells

Immunohistochemical stainings for MAC3 and CD3 were increased in KO+MI+PBS compared to KO+Sham+PBS. In contrast to the results from WT (**Figure 5**), αGC did not alter them (**Supplemental Figure 1**). MPO positive cells were not detected in the LV tissue from either group of mice (data not shown). MCP-1 and RANTES were increased in KO+MI+PBS compared to KO+Sham+PBS, and were not affected by αGC (**Supplemental Figure 2A and B)**. There was no difference in TNF-α and IL-10 in the LV tissue from either group of mice (**Supplemental Figure 2C and D**). These data suggest that αGC did not directly activate other inflammatory cell, induce chemokines, and produce inflammatory cytokines.

Discussion

The present study demonstrated that the activation of iNKT cells by αGC improved survival and ameliorated LV remodeling and failure after MI in mice, accompanied by the decreases in interstitial fibrosis, cardiomyocyte hypertrophy and apoptosis. Furthermore, the enhanced expression of IL-10 by αGC is involved in these effects. This is the first report to provide direct evidence for increased iNKT cells in MI and the inhibitory effects of their activation on the development of post-MI HF.

Chronic infiltration of inflammatory cells including iNKT cells in Post-MI heart

In the setting of acute MI, the infiltration of inflammatory cells such as neutrophils, macrophages, and lymphocytes is a physiological repair process and beneficial removing dead cardiomyocytes and leading to the repair and scar formation of infarcted area.[18] However, the chronic inflammatory response in the non-infarcted area causes the further myocardial damage and fibrosis, leading to the progressive impairment of cardiac function.[19] We have previously demonstrated that anti-MCP-1 gene therapy improved survival and attenuated LV dilation and contractile dysfunction, which was associated with the decreases in macrophage infiltration and gene expression of myocardial inflammatory cytokines.[2] Therefore, chronic myocardial inflammation plays a crucial role on LV remodeling and failure after MI. However, the precise role of various inflammatory cells and chemokines in this disease process has not been fully elucidated. iNKT cells are specialized lineage of T cells that recognize glycolipid antigens presented by the MHC class I-like molecule CD1d. The iNKT cells mediate various functions rapidly by producing a mixture of T_H1 and T_H2 cytokines and vast array of chemokines.[6] Thus, iNKT cells can function as a bridge between the innate and adaptive immune systems, and orchestrate tissue inflammation. However, to our knowledge, there has been only one paper by Olson et al. reported the presence of iNKT cells in cardiac tissue obtained from acute Lyme carditis model.[20] Therefore, the present study was the first that demonstrated the increased infiltration of iNKT cells in post-MI hearts (**Figure 1**).

Effects of the activation of iNKT cells by αGC in Post-MI heart

The most important finding of this study was that the activation of iNKT cells by αGC improved survival and attenuated LV remodeling and failure after MI (**Figures 2 and 3, Table 1**). The beneficial effects of αGC were not attributable to its MI size-sparing effect, because the infarct size calculated as % LV circumference was comparable between MI+PBS and MI+αGC mice. Furthermore, its effects might not be attributable to those on hemodynamics, because blood pressure and heart rate were not altered (**Table 1**). αGC, a glycosphingolipid, is a well-known iNKT cell receptor ligand that can specifically activate iNKT cells.[13] It has been demonstrated that iNKT cells expand dramatically

2-3 days after *in vivo* treatment with αGC, and return to the baseline level by approximately 9 days after treatment.[21, 22] Moreover, the effects of iNKT cell stimulation may differ according to the timing of αGC administration. In the model of experimental autoimmune encephalomyelitis, early immunization with αGC protected against this disease, whereas later immunization potentiated it.[23] In the present study, αGC injection significantly enhanced iNKT cell infiltration (**Figure 1**) and could effectively ameliorate post-MI LV remodeling and failure (**Figures 2 and 3**).

Role of IL-10 in the inhibitory effects of iNKT cell activation by αGC

Another important finding of the present study was that the enhanced expression of IL-10 was involved in the inhibitory effects of iNKT cell activation against LV remodeling and failure (**Table 2**). These results are consistent with the previous findings that the therapeutic effects of αGC against T_H1-like autoimmune diseases include two mechanisms such as a shift from T_H1 toward a T_H2 pattern[9-11, 23] and the induction of immunosuppresive cytokine IL-10.[9, 11, 12] The present study demonstrated that IL-10 was increased in non-infarcted LV from sham and MI animals in association with an increase in iNKT cells after the treatment with αGC at 7 days (**Figure 6C and D**). Interestingly, the enhanced expression of IL-10 gene by αGC persisted only in MI mice. These changes of IL-10 gene expression (**Figure 6D**) completely corresponded to those of iNKT cells (**Figure 1B**). Moreover, the inhibitory effects of αGC on LV remodeling and HF were reversed by anti-IL-10 receptor antibody and the treatment with only anti-IL-10 antibody of MI mice did not affect LV remodeling and HF (**Table 2**). Therefore, these data suggest that IL-10 is not associated with the development of LV remodeling and HF after MI without αGC, and IL-10 is involved in the beneficial effects of iNKT cell activation against post-MI remodeling and failure. These findings were consistent with a recent study by Krishnamurthy et al, in which LV dimension and function by echocardiography after MI did not differ between wild-type and IL-10-null mice.[24]

Possible mechanisms of IL-10 for the attenuation of LV remodeling

IL-10 can inhibit the production of proinflammatory cytokines by macrophages and T_H1 cells,[25, 26] and directly promote the death of inflammatory cells.[27] Furthermore, beyond its suppressive effects on inflammatory gene synthesis, IL-10 also regulates extracellular matrix[28] and angiogenesis.[29] In the present study, the activation of iNKT cells by αGC decreased cardiac myocyte hypertrophy and apoptosis, and inhibited interstitial fibrosis possibly through inhibiting the zymographic MMP-2 level in non-infarcted LV (**Figure 4**). MMP-2 is ubiquitously distributed in cardiac myocytes and fibroblasts, and has been shown to play a crucial role in the development of cardiac remodeling after MI.[30] Theoretically, an increase in MMP activity would result in a decrease in the MMP substrate, collagens, whereas an inhibition of MMP would result in an increase in collagens. However, our previous study showed that the selective disruption of the MMP-2 gene attenuated interstitial fibrosis after MI.[30]

Therefore, the decrease in zymographic MMP-2 level by αGC might be involved in the attenuation of interstitial fibrosis in our model. On the other hand, MMP-9 is mainly expressed in infiltrating inflammatory cells such as neutrophils and T lymphocytes. Previous paper showed that subcutaneous injection of recombinant IL-10 suppressed inflammation and attenuated LV remodeling after MI in mice by inhibiting fibrosis via suppression of HuR/MMP-9 and by enhancing capillary density through the activation of STAT3.[31] Moreover, the previous study by Burchfield et al showed that IL-10 from transplanted bone marrow mononuclear cells contributed to cardiac protection after MI in association with a decrease in T lymphocyte accumulation, reactive hypertrophy, and myocardial collagen deposition.[32] However, in the present study, zymographic MMP-9 level was not affected by αGC, which was consistent with the infiltration of lymphocyte observed by immunohistochemical staining for CD3 (**Figure 5**). We also measured the protein levels of HuR/MMP-9 or STAT3 in the non-infarcted LV. However, these protein levels were not affected by αGC (data not shown).

Role of other inflammatory cells and cytokines

In agreement with the increase in macrophage infiltration by αGC, MCP-1 gene expression was increased. αGC increased not only M1 macrophage but also M2 macrophage, which tune inflammatory responses and promote tissue repair.[33] Therefore, the increase in M2 macrophage might neutralize the effect of the increased M1 macrophage and MCP-1. The present study also showed that TNF-α was increased in non-infarcted LV from MI+αGC **(Figure 6)**. TNF-α is a proinflammatory cytokine considered to be cardiotoxic and induce LV dysfunction.[34] However, in contrast, TNF-α has also protective effects during the maladaptive transition to HF.[35] Indeed, the treatment of patients with HF with either soluble TNF receptor (RENEWAL) or an anti-TNF antibody (ATTACH) could not show clinical benefits.[36, 37] Therefore, the increase in TNF-α by αGC would not necessarily lead to the aggravation of LV remodeling.

Limitations

There are several limitations to be acknowledged in the present study. First, we could not directly demonstrate the location of iNKT cells by the immunohistochemical analysis using biotinylated CD1d dimer (BD Bioscience) with loading of αGC according to the previous report by Kamijyuku et al.[38] We tried the double immunohistochemical staining using antibodies for anti-armenian hamster TCR-β-PE (BD Bioscience) and anti-mouse NK 1.1-APC (BD Bioscience) according to the newly published paper.[39] Furthermore, we also performed in situ hybridization using Digoxigenin-labeled DNA probes for mouse Vα14Jα18. Unfortunately, however, we could not detect iNKT cells *in situ* in the heart. Even though we defined iNKT cells within the heart by using the gene expression as well as the flow cytometric analysis, further studies are needed to overcome some technical difficulties of *in situ* detection and clarify this important issue. Second, the underlying

mechanisms responsible for the activation of iNKT cells after MI remain to be established. To date, the endogenous ligand for iNKT cells has not been known. Based on our results using αGC, a glycosphingolipid, sphingolipid ceramide may be a crucial intermediate, since ceramide has been shown to be synthesized by long-chain fatty acids and actually increased in the heart after coronary microembolization.[40] Third, the source of IL-10 production after the stimulation of αGC remains to be determined. IL-10 has been shown to be produced by iNKT cells themselves upon exogenous stimulation.[41] In addition, IL-10 can be expressed and secreted from macrophages activated by iNKT cells.[42, 43] In the present study, the activation of iNKT cells by αGC injection increased the infiltration of macrophage in sham and MI mice at 7 days, however, there was no difference in it between MI+PBS and MI+αGC at 28 days (**Figure 6**). Therefore, the main source of IL-10 production at later phase of αGC injection would be the cells other than macrophages.

In conclusion, iNKT cells have a protective effect on LV remodeling and failure after MI via enhanced IL-10 expression. Therefore, therapies designed to activate iNKT cells may be beneficial against the development of post-MI heart failure.

Acknowledgements

We thank Kaoruko Kawai, Akiko Aita, and Miwako Fujii for excellent technical assistance.

Sources of Fundings

This study was supported by grants from the Ministry of Education, Science, and Culture (17390223, 20590854, 20117004, 21390236), and Hokkaido Heart Association Grant for Research.

Disclosures

None

References

1. Pfeffer MA, Braunwald E. Ventricular remodeling after myocardial infarction. Experimental observations and clinical implications. *Circulation.* 1990;81:1161-1172.
2. Hayashidani S, Tsutsui H, Shiomi T, Ikeuchi M, Matsusaka H, Suematsu N, Wen J, Egashira K, Takeshita A. Anti-monocyte chemoattractant protein-1 gene therapy attenuates left ventricular remodeling and failure after experimental myocardial infarction. *Circulation.* 2003;108:2134-2140.
3. Varda-Bloom N, Leor J, Ohad DG, Hasin Y, Amar M, Fixler R, Battler A, Eldar M, Hasin D. Cytotoxic T lymphocytes are activated following myocardial infarction and can recognize and kill healthy myocytes in vitro. *J Mol Cell Cardiol.* 2000;32:2141-2149.
4. Shiomi T, Tsutsui H, Hayashidani S, Suematsu N, Ikeuchi M, Wen J, Ishibashi M, Kubota T, Egashira K, Takeshita A. Pioglitazone, a peroxisome proliferator-activated receptor-gamma agonist, attenuates left ventricular remodeling and failure after experimental myocardial infarction. *Circulation.* 2002;106:3126-3132.
5. Kaikita K, Hayasaki T, Okuma T, Kuziel WA, Ogawa H, Takeya M. Targeted deletion of CC chemokine receptor 2 attenuates left ventricular remodeling after experimental myocardial infarction. *Am J Pathol.* 2004;165:439-447.
6. Matsuda JL, Mallevaey T, Scott-Browne J, Gapin L. CD1d-restricted iNKT cells, the 'Swiss-Army knife' of the immune system. *Curr Opin Immunol.* 2008;20:358-368.
7. Nakai Y, Iwabuchi K, Fujii S, Ishimori N, Dashtsoodol N, Watano K, Mishima T, Iwabuchi C, Tanaka S, Bezbradica JS, Nakayama T, Taniguchi M, Miyake S, Yamamura T, Kitabatake A, Joyce S, Van Kaer L, Onoe K. Natural killer T cells accelerate atherogenesis in mice. *Blood.* 2004;104:2051-2059.
8. Ohmura K, Ishimori N, Ohmura Y, Tokuhara S, Nozawa A, Horii S, Andoh Y, Fujii S, Iwabuchi K, Onoe K, Tsutsui H. Natural killer T cells are involved in adipose tissues inflammation and glucose intolerance in diet-induced obese mice. *Arterioscler Thromb Vasc Biol.* 2010;30:193-199.
9. Hong S, Wilson MT, Serizawa I, Wu L, Singh N, Naidenko OV, Miura T, Haba T, Scherer DC, Wei J, Kronenberg M, Koezuka Y, Van Kaer L. The natural killer T-cell ligand alpha-galactosylceramide prevents autoimmune diabetes in non-obese diabetic mice. *Nat Med.* 2001;7:1052-1056.
10. Sharif S, Arreaza GA, Zucker P, Mi QS, Sondhi J, Naidenko OV, Kronenberg M, Koezuka Y, Delovitch TL, Gombert JM, Leite-De-Moraes M, Gouarin C, Zhu R, Hameg A, Nakayama T, Taniguchi M, Lepault F, Lehuen A, Bach JF, Herbelin A. Activation of natural killer T cells by alpha-galactosylceramide treatment prevents the onset and recurrence of autoimmune Type

1 diabetes. *Nat Med.* 2001;7:1057-1062.

11. Furlan R, Bergami A, Cantarella D, Brambilla E, Taniguchi M, Dellabona P, Casorati G, Martino G. Activation of invariant NKT cells by alphaGalCer administration protects mice from MOG35-55-induced EAE: critical roles for administration route and IFN-gamma. *Eur J Immunol.* 2003;33:1830-1838.
12. Miellot A, Zhu R, Diem S, Boissier MC, Herbelin A, Bessis N. Activation of invariant NK T cells protects against experimental rheumatoid arthritis by an IL-10-dependent pathway. *Eur J Immunol.* 2005;35:3704-3713.
13. Van Kaer L. alpha-Galactosylceramide therapy for autoimmune diseases: prospects and obstacles. *Nat Rev Immunol.* 2005;5:31-42.
14. Kinugawa S, Tsutsui H, Hayashidani S, Ide T, Suematsu N, Satoh S, Utsumi H, Takeshita A. Treatment with dimethylthiourea prevents left ventricular remodeling and failure after experimental myocardial infarction in mice: role of oxidative stress. *Circ Res.* 2000;87:392-398.
15. Namba T, Tsutsui H, Tagawa H, Takahashi M, Saito K, Kozai T, Usui M, Imanaka-Yoshida K, Imaizumi T, Takeshita A. Regulation of fibrillar collagen gene expression and protein accumulation in volume-overloaded cardiac hypertrophy. *Circulation.* 1997;95:2448-2454.
16. Leuschner F, Panizzi P, Chico-Calero I, Lee WW, Ueno T, Cortez-Retamozo V, Waterman P, Gorbatov R, Marinelli B, Iwamoto Y, Chudnovskiy A, Figueiredo JL, Sosnovik DE, Pittet MJ, Swirski FK, Weissleder R, Nahrendorf M. Angiotensin-converting enzyme inhibition prevents the release of monocytes from their splenic reservoir in mice with myocardial infarction. *Circ Res.* 2010;107:1364-1373.
17. Kawano T, Cui J, Koezuka Y, Toura I, Kaneko Y, Motoki K, Ueno H, Nakagawa R, Sato H, Kondo E, Koseki H, Taniguchi M. CD1d-restricted and TCR-mediated activation of valpha14 NKT cells by glycosylceramides. *Science.* 1997;278:1626-1629.
18. Blankesteijn WM, Creemers E, Lutgens E, Cleutjens JP, Daemen MJ, Smits JF. Dynamics of cardiac wound healing following myocardial infarction: observations in genetically altered mice. *Acta Physiol Scand.* 2001;173:75-82.
19. Frangogiannis NG, Smith CW, Entman ML. The inflammatory response in myocardial infarction. *Cardiovasc Res.* 2002;53:31-47.
20. Olson CM, Jr., Bates TC, Izadi H, Radolf JD, Huber SA, Boyson JE, Anguita J. Local production of IFN-gamma by invariant NKT cells modulates acute Lyme carditis. *J Immunol.* 2009;182:3728-3734.
21. Crowe NY, Uldrich AP, Kyparissoudis K, Hammond KJ, Hayakawa Y, Sidobre S, Keating R, Kronenberg M, Smyth MJ, Godfrey DI. Glycolipid antigen drives rapid expansion and sustained cytokine production by NK T cells. *J Immunol.* 2003;171:4020-4027.

22. Wilson MT, Johansson C, Olivares-Villagomez D, Singh AK, Stanic AK, Wang CR, Joyce S, Wick MJ, Van Kaer L. The response of natural killer T cells to glycolipid antigens is characterized by surface receptor down-modulation and expansion. *Proc Natl Acad Sci U S A.* 2003;100:10913-10918.
23. Jahng AW, Maricic I, Pedersen B, Burdin N, Naidenko O, Kronenberg M, Koezuka Y, Kumar V. Activation of natural killer T cells potentiates or prevents experimental autoimmune encephalomyelitis. *J Exp Med.* 2001;194:1789-1799.
24. Krishnamurthy P, Lambers E, Verma S, Thorne T, Qin G, Losordo DW, Kishore R. Myocardial knockdown of mRNA-stabilizing protein HuR attenuates post-MI inflammatory response and left ventricular dysfunction in IL-10-null mice. *Faseb J.*24:2484-2494.
25. Fiorentino DF, Zlotnik A, Vieira P, Mosmann TR, Howard M, Moore KW, O'Garra A. IL-10 acts on the antigen-presenting cell to inhibit cytokine production by Th1 cells. *J Immunol.* 1991;146:3444-3451.
26. Frangogiannis NG, Mendoza LH, Lindsey ML, Ballantyne CM, Michael LH, Smith CW, Entman ML. IL-10 is induced in the reperfused myocardium and may modulate the reaction to injury. *J Immunol.* 2000;165:2798-2808.
27. Wang P, Wu P, Siegel MI, Egan RW, Billah MM. Interleukin (IL)-10 inhibits nuclear factor kappa B (NF kappa B) activation in human monocytes. IL-10 and IL-4 suppress cytokine synthesis by different mechanisms. *J Biol Chem.* 1995;270:9558-9563.
28. Lacraz S, Nicod LP, Chicheportiche R, Welgus HG, Dayer JM. IL-10 inhibits metalloproteinase and stimulates TIMP-1 production in human mononuclear phagocytes. *J Clin Invest.* 1995;96:2304-2310.
29. Silvestre JS, Mallat Z, Duriez M, Tamarat R, Bureau MF, Scherman D, Duverger N, Branellec D, Tedgui A, Levy BI. Antiangiogenic effect of interleukin-10 in ischemia-induced angiogenesis in mice hindlimb. *Circ Res.* 2000;87:448-452.
30. Hayashidani S, Tsutsui H, Ikeuchi M, Shiomi T, Matsusaka H, Kubota T, Imanaka-Yoshida K, Itoh T, Takeshita A. Targeted deletion of MMP-2 attenuates early LV rupture and late remodeling after experimental myocardial infarction. *Am J Physiol Heart Circ Physiol.* 2003;285:H1229-1235.
31. Krishnamurthy P, Rajasingh J, Lambers E, Qin G, Losordo DW, Kishore R. IL-10 inhibits inflammation and attenuates left ventricular remodeling after myocardial infarction via activation of STAT3 and suppression of HuR. *Circ Res.* 2009;104:e9-18.
32. Burchfield JS, Iwasaki M, Koyanagi M, Urbich C, Rosenthal N, Zeiher AM, Dimmeler S. Interleukin-10 from transplanted bone marrow mononuclear cells contributes to cardiac protection after myocardial infarction. *Circ Res.* 2008;103:203-211.
33. Mantovani A, Sica A, Locati M. Macrophage polarization comes of age. *Immunity.*

2005;23:344-346.

34. Kubota T, McTiernan CF, Frye CS, Slawson SE, Lemster BH, Koretsky AP, Demetris AJ, Feldman AM. Dilated cardiomyopathy in transgenic mice with cardiac-specific overexpression of tumor necrosis factor-alpha. *Circ Res.* 1997;81:627-635.
35. Wang X, Oka T, Chow FL, Cooper SB, Odenbach J, Lopaschuk GD, Kassiri Z, Fernandez-Patron C. Tumor necrosis factor-alpha-converting enzyme is a key regulator of agonist-induced cardiac hypertrophy and fibrosis. *Hypertension.* 2009;54:575-582.
36. Mann DL, McMurray JJ, Packer M, Swedberg K, Borer JS, Colucci WS, Djian J, Drexler H, Feldman A, Kober L, Krum H, Liu P, Nieminen M, Tavazzi L, van Veldhuisen DJ, Waldenstrom A, Warren M, Westheim A, Zannad F, Fleming T. Targeted anticytokine therapy in patients with chronic heart failure: results of the Randomized Etanercept Worldwide Evaluation (RENEWAL). *Circulation.* 2004;109:1594-1602.
37. Chung ES, Packer M, Lo KH, Fasanmade AA, Willerson JT. Randomized, double-blind, placebo-controlled, pilot trial of infliximab, a chimeric monoclonal antibody to tumor necrosis factor-alpha, in patients with moderate-to-severe heart failure: results of the anti-TNF Therapy Against Congestive Heart Failure (ATTACH) trial. *Circulation.* 2003;107:3133-3140.
38. Kamijuku H, Nagata Y, Jiang X, Ichinohe T, Tashiro T, Mori K, Taniguchi M, Hase K, Ohno H, Shimaoka T, Yonehara S, Odagiri T, Tashiro M, Sata T, Hasegawa H, Seino KI. Mechanism of NKT cell activation by intranasal coadministration of alpha-galactosylceramide, which can induce cross-protection against influenza viruses. *Mucosal Immunol.* 2008;1:208-218.
39. Barral P, Sanchez-Nino MD, van Rooijen N, Cerundolo V, Batista FD. The location of splenic NKT cells favours their rapid activation by blood-borne antigen. *Embo J.*31:2378-2390.
40. Thielmann M, Dorge H, Martin C, Belosjorow S, Schwanke U, van De Sand A, Konietzka I, Buchert A, Kruger A, Schulz R, Heusch G. Myocardial dysfunction with coronary microembolization: signal transduction through a sequence of nitric oxide, tumor necrosis factor-alpha, and sphingosine. *Circ Res.* 2002;90:807-813.
41. Sonoda KH, Faunce DE, Taniguchi M, Exley M, Balk S, Stein-Streilein J. NK T cell-derived IL-10 is essential for the differentiation of antigen-specific T regulatory cells in systemic tolerance. *J Immunol.* 2001;166:42-50.
42. Platzer C, Docke W, Volk H, Prosch S. Catecholamines trigger IL-10 release in acute systemic stress reaction by direct stimulation of its promoter/enhancer activity in monocytic cells. *J Neuroimmunol.* 2000;105:31-38.
43. Troidl C, Mollmann H, Nef H, Masseli F, Voss S, Szardien S, Willmer M, Rolf A, Rixe J, Troidl K, Kostin S, Hamm C, Elsasser A. Classically and alternatively activated macrophages contribute to tissue remodelling after myocardial infarction. *J Cell Mol Med.*

2009;13:3485-3496.

Table 1. Echocardiography, Hemodynamics, and Organ Weights in Experiment 2

	Sham+PBS	Sham+αGC	MI+PBS	MI+αGC
N	10	10	10	16
Echocardiography				
Heart rate, bpm	522±10	522±12	531±16	520±13
LVEDD, mm	3.4±0.1	3.4±0.04	5.4±0.1*	5.0±0.1*†
LVESD, mm	2.1±0.03	2.1±0.04	4.5±0.1*	4.1±0.1*†
FS, %	38.2±0.7	38.3±0.6	16.5±0.6*	18.8±0.6*†
AWT, mm	0.63±0.01	0.62±0.01	0.31±0.01*	0.30±0.01*
PWT, mm	0.68±0.02	0.68±0.01	0.97±0.01*	0.96±0.02*
Hemodynamics				
Heart rate, /min	507±9	499±9	485±23	495±11
Mean AoP, mmHg	78.1±2	77.7±2	75.0±3	79.3±1
LVEDP, mmHg	1.7±0.3	2.3±0.1	10.7±1.1*	6.6±0.6*†
LV +dP/dt, mmHg/s	15625±623	14972±398	7352±697*	9386±476*†
LV -dP/dt, mmHg/s	9983±697	9130±691	5045±482*	5861±286*
Organ Weights				
Body wt, g	25.1±0.3	24.9±0.2	24.5±0.4	24.8±0.3
Heart wt/Body wt, mg/g	4.6±0.1	4.5±0.1	6.8±0.2*	6.1±0.1*†
Lung wt/Body wt, mg/g	5.2±0.03	5.2±0.1	7.2±0.7*	5.9±0.2†
Infarct size, %	-	-	56±2	55±1

LVEDD, left ventricular end-diastolic diameter; LVESD, left ventricular end-systolic diameter; FS, fractional shortening; AWT, anterior wall thickness; PWT, posterior wall thickness; AoP, aortic pressure; LVEDP, left ventricular end-diastolic pressure; wt, weight. Data are mean ± SEM. *P<0.05 vs. Sham+PBS, †P<0.05 vs. MI+PBS.

Table 2. Echocardiography, Hemodynamics, and Organ Weights in Experiment 3

	MI+αGC	MI+ anti-IL-10 receptor antibody	MI+αGC+ anti-IL-10 receptor antibody
N	8	8	8
Echocardiography			
Heart rate, bpm	516±18	519±16	510±18
LVEDD, mm	4.8±0.1	5.4±0.1*	5.4±0.1*
LVESD, mm	3.9±0.1	4.6±0.1*	4.6±0.1*
FS, %	19±0.8	14.5±0.7*	15.4±0.7*
AWT, mm	0.30±0.01	0.37±0.06	0.35±0.06
PWT, mm	0.98±0.02	1.02±0.02	0.99±0.04
Hemodynamics			
Heart rate, /min	518±16	487±17	515±22
Mean AoP, mmHg	86±3	81±4	82±2
LVEDP, mmHg	5.4±0.8	10.8±0.7*	11.4±3.3*
LV +dP/dt, mmHg/s	10441±661	6555±1031	7719±1284
LV -dP/dt, mmHg/s	6847±569	4119±364	5774±1236
Organ Weights			
Body wt, g	25.2±0.5	24.7±1.3	25.8±0.6
Heart wt/Body wt, mg/g	6.3±0.3	8.8±0.9	6.9±0.5
Lung wt/Body wt, mg/g	5.5±0.1	10.9±2.1*	7.9±1.0*
Infarct size, %	56±2	54±2	56±4

LVEDD, left ventricular end-diastolic diameter; LVESD, left ventricular end-systolic diameter; FS, fractional shortening; AWT, anterior wall thickness; PWT, posterior wall thickness; AoP, aortic pressure; LVEDP, left ventricular end-diastolic pressure; wt, weight. Data are mean ± SEM. *P<0.05 vs. MI+αGC.

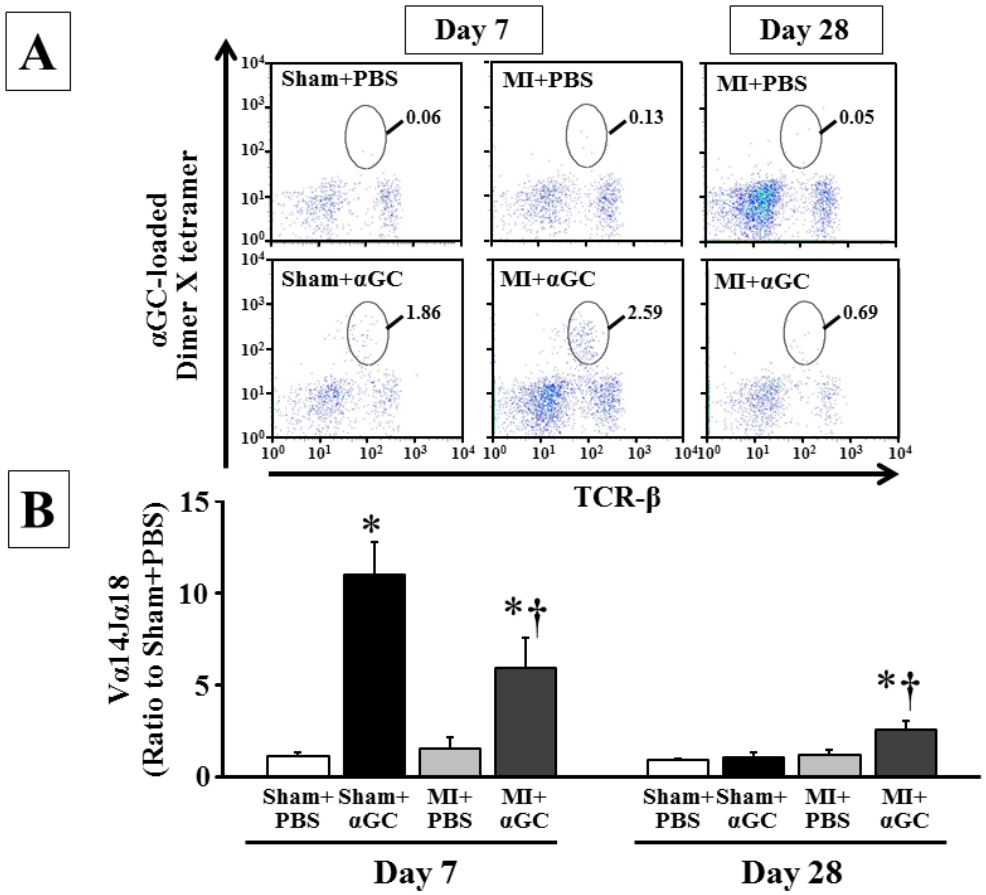

Figure 1. (A) Representative flow cytometric assessment of cardiac mononuclear cells obtained from Sham+PBS, Sham+αGC, MI+PBS, and MI+αGC at day 7 and 28. Cardiac mononuclear cells from 5 different mice for each group were pooled and analyzed. The experiments were performed 3 times. iNKT cells were gated as the αGC-loaded dimer X tetramer^{+}TCR-β^{+} population. The inset numbers are a percentage of the gated region of the samples. (B) Gene expression of Vα14/Jα18 in non-infarcted LV from sham+PBS, sham+αGC, MI+PBS and MI+αGC 7 days (n=6) and 28 days (n=4) after surgery. They were normalized to GAPDH gene expression and expressed as ratio to sham+PBS values. Data are expressed as means ± SE. **P*<0.05 vs. Sham+PBS, †*P*<0.05 vs. MI+PBS.

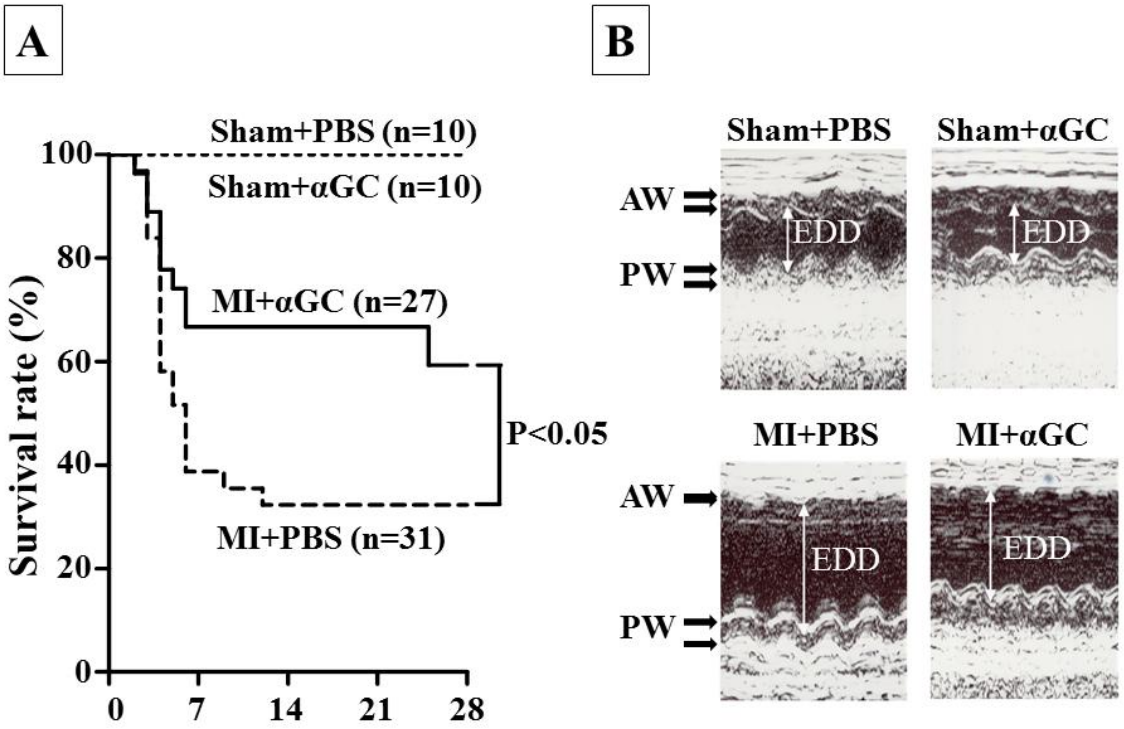

Figure 2. (A) Percent survival of Sham+PBS (n=10), Sham+αGC (n=10), MI+PBS (n=31) and MI+αGC (n=27) mice shown by Kaplan-Meier method. (B) Representative M-mode echocardiographic images obtained from sham+PBS, sham+αGC, MI+PBS and MI+αGC. AW indicates anterior wall; PW, posterior wall; EDD, end-diastolic diameter.

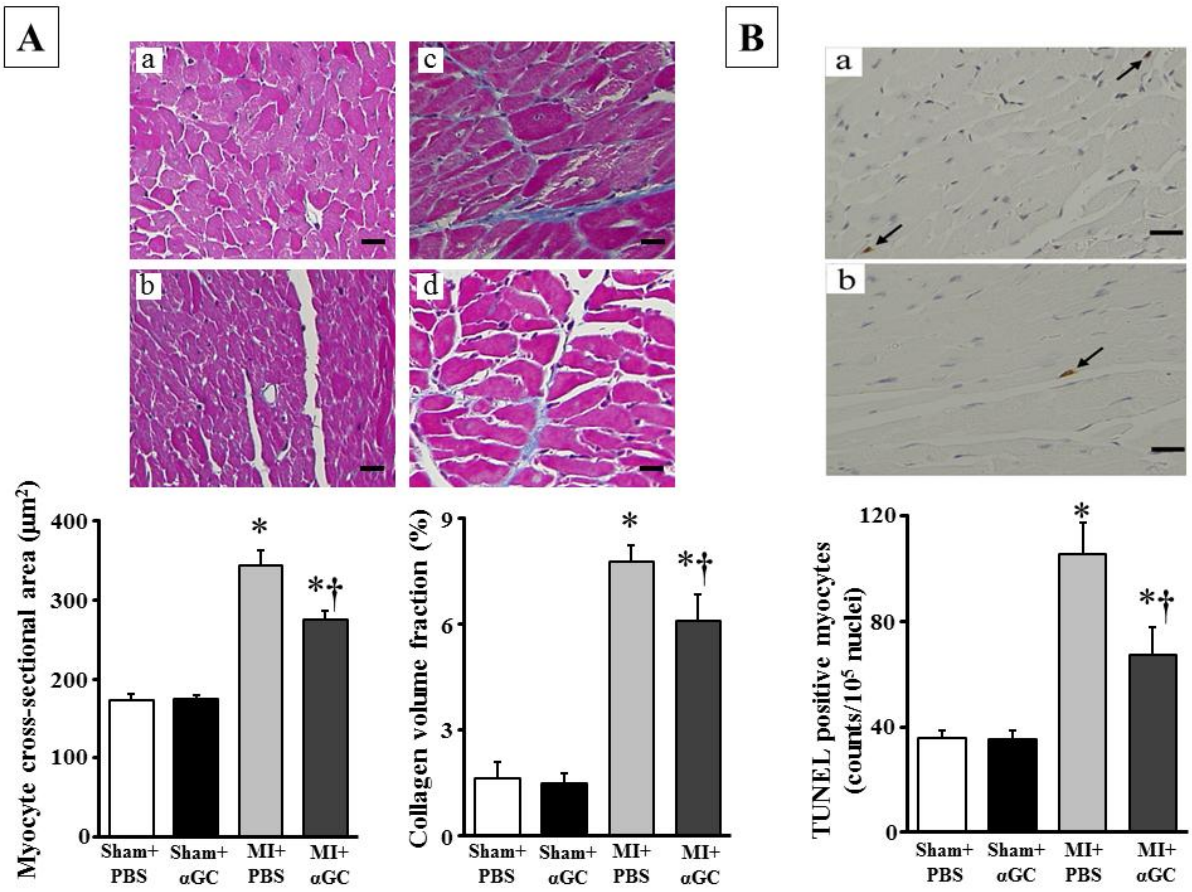

Figure 3. (A) Representative high-power photomicrographs of LV cross-sections stained with Masson's trichrome from sham+PBS (a), sham+αGC (b), MI+PBS (c) and MI+αGC (d) and summary data of myocyte cross-sectional area and collagen volume fraction in 4 groups of mice (n=6). Scale bar, 20 μm. (B) Representative photomicrographs TUNEL staining of LV sections from MI+PBS (a) and MI+αGC (b) and summary data for the number of TUNEL-positive cells in the non-infarcted LV (n=6). Scale bar, 20 μm. Data are expressed as means ± SE. **P*<0.05 vs. Sham+PBS, †*P*<0.05 vs.

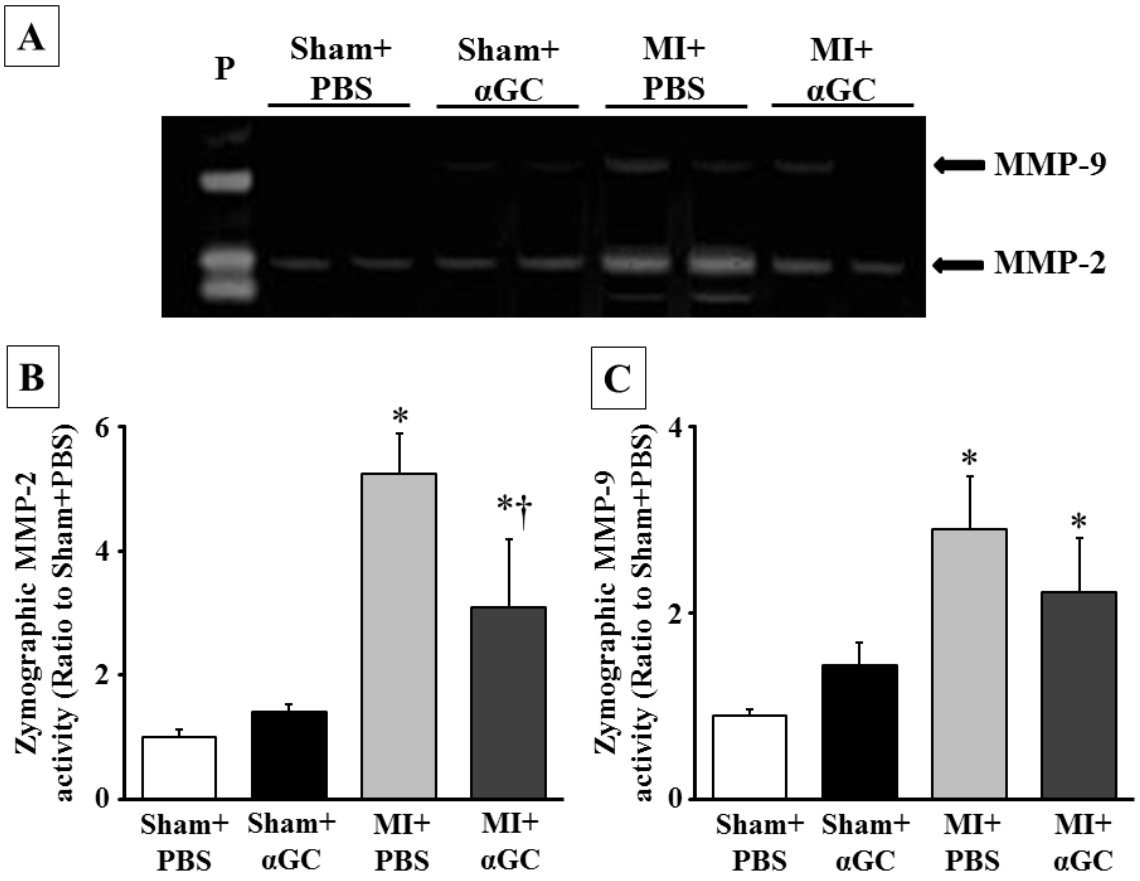

Figure 4. Representative LV zymographic MMP-2 and MMP-9 activities in non-infarcted LV at 7 days after surgery (A) and their densitometric analysis (B and C; n=5 for each). P, positive control. Data are expressed as means ± SE. **P*<0.05 vs. Sham+PBS, †*P*<0.05 vs. MI+PBS.

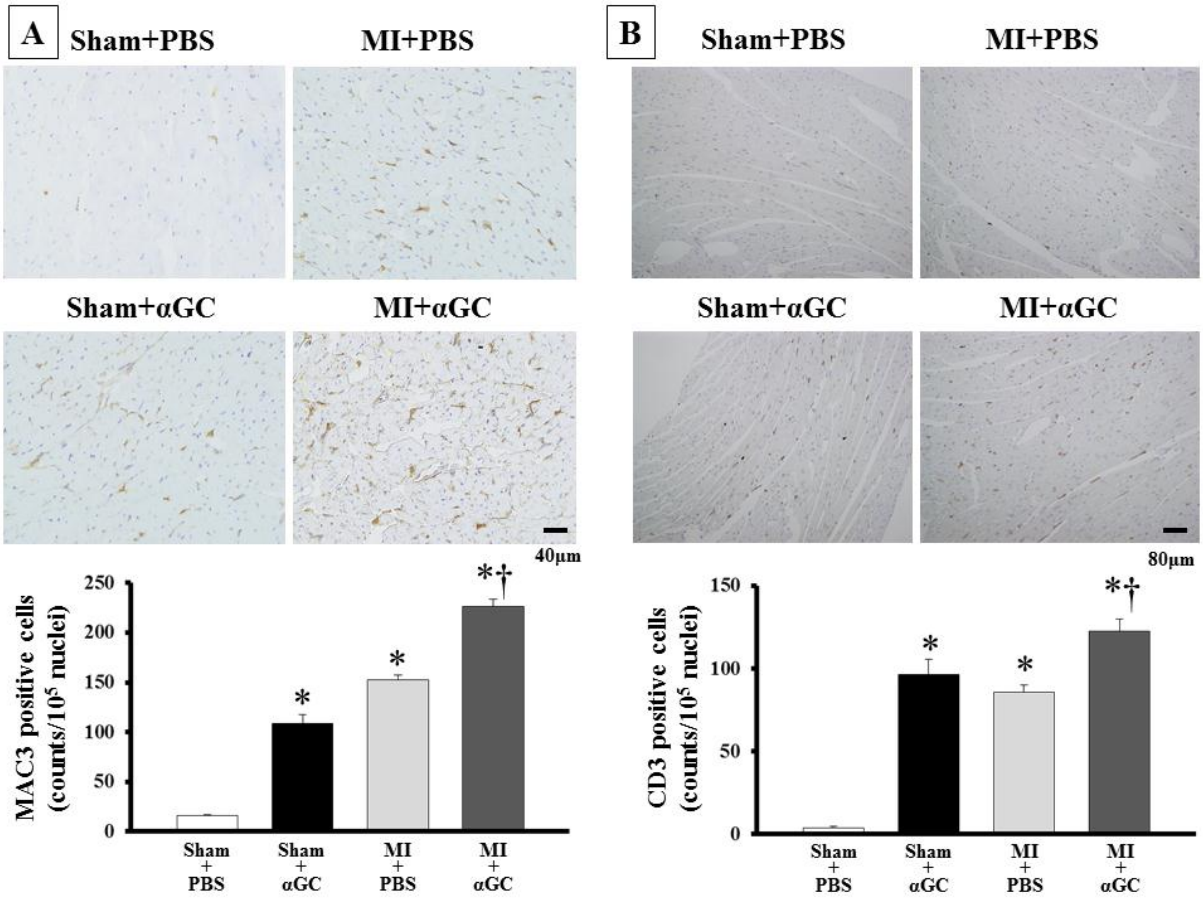

Figure 5. Representative photomicrographs of LV cross-sections stained with (**A, upper panel**) anti MAC3 and (**B, upper panel**) anti CD3 in Sham+PBS, Sham+αGC, MI+PBS and MI+αGC. Summary data of the numbers of (**A, lower panel**) MAC3 and (**B, lower panel**) CD3 positive cells in the LV (n=4-8 for each). Data are means±SE. **P*<0.05 vs. Sham+PBS, †*P*<0.05 vs. MI+PBS.

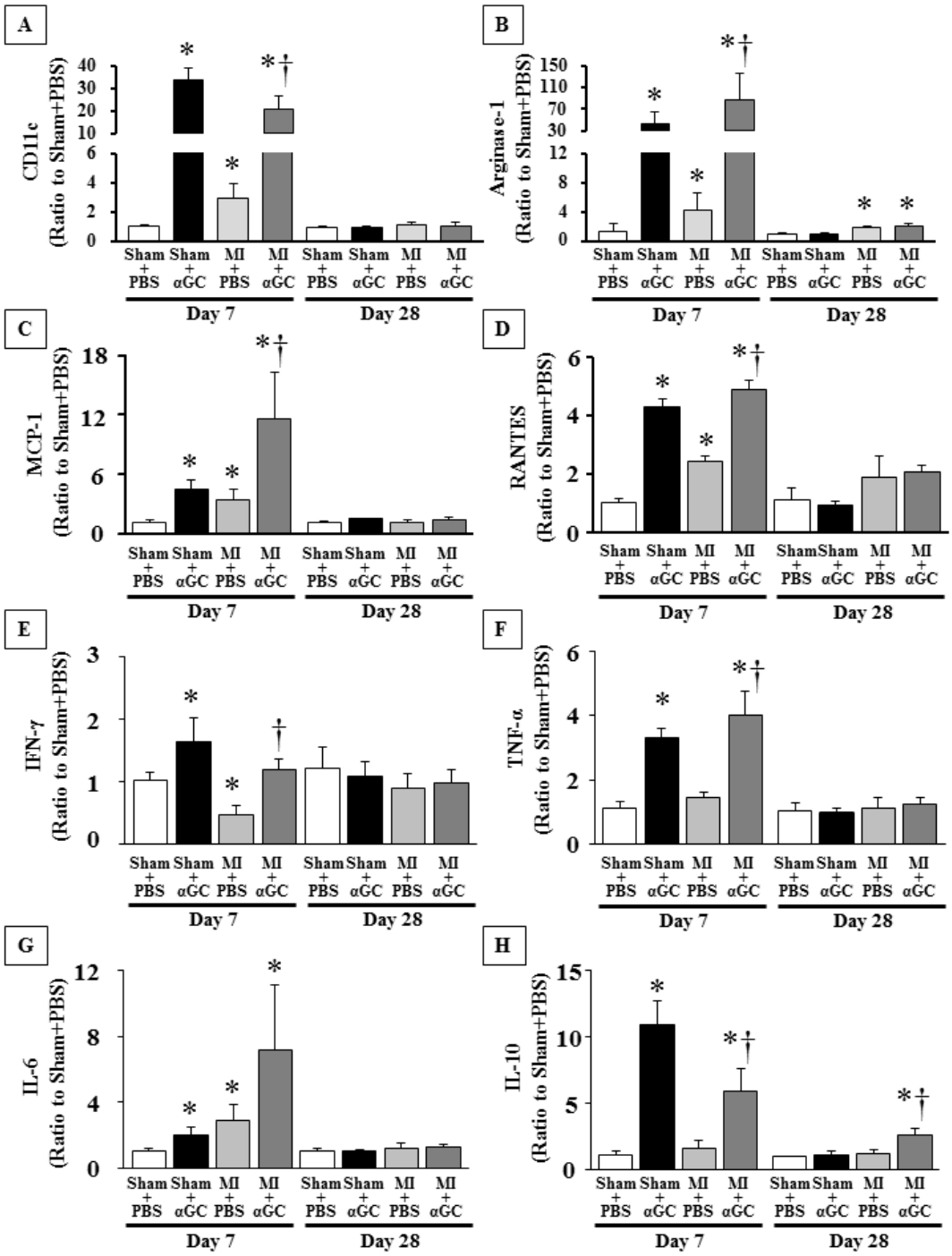

Figure 6. Quantitative analysis of gene expression of CD11c (A), Arginase (B), MCP-1 (C), RANTES (D), IFN-γ (E), TNF-α (F), IL-6 (G), and IL-10 (H) in the non-infarcted LV at day 7 (n=6) and 28 (n=4) after surgery. Gene expression was normalized to GAPDH and depicted as the ratio to Sham+PBS. Data are expressed as means ± SE. **P*<0.05 vs. Sham+PBS, †*P*<0.05 vs. MI+PBS.